Identification of newly observed singly charmed baryons using the relativistic flux tube model

Pooja Jakhad,[1] Juhi Oudichhya,[1] Keval Gandhi,[2] and Ajay Kumar Rai[1,*]

[1]*Department of Physics, Sardar Vallabhbhai National Institute of Technology, Surat, Gujarat-395007, India*

[2]*Department of Computer Science and Engineering, Institute of Advanced Research, Gandhinagar, Gujarat-382426, India*

(Received 22 January 2023; accepted 9 June 2023; published 12 July 2023)

We calculate the mass spectra of Λ_c, Ξ_c, Σ_c, Ξ_c', and Ω_c baryons in the framework of a quark-diquark configuration using the relativistic flux tube model. The spin-dependent interactions are included in the j-j coupling scheme to find the complete mass spectra. We satisfactorily describe the known singly charmed baryons in a quark-diquark configuration. The possible spin-parity J^P quantum numbers are assigned to several experimentally observed states. Furthermore, some useful mass predictions are given for more excited states that are reasonably consistent with other model predictions for lower excited states. From the obtained results, the Regge trajectories for these singly charmed baryons are constructed in the (J, M^2) plane, and the properties like linearity, parallelism, and equidistance are verified. Also, these predictions should be tested in future experiments.

DOI: 10.1103/PhysRevD.108.014011

I. INTRODUCTION

Singly charmed baryons provide the best environment to investigate the dynamics of light quarks in the presence of a heavy charm quark. In recent years, a significant experimental effort has been made to measure the singly charmed baryons. Many experiment groups such as LHCb, Belle, *BABAR*, and CLEO have provided data and are expected to produce more precise results in the near future [1].

The latest review of particle physics by the Particle Data Group (PDG) [1] confirms the six states of the Λ_c baryon with their respective spin and parity (see Table I), but $\Lambda_c(2765)^+/\Sigma_c(2765)^+$ is still a controversial state. It was first observed in the $\Lambda_c\pi^+\pi^-$ decay channel by the CLEO Collaboration [2] and later confirmed by the Belle Collaboration in the $\Sigma_c\pi$ decay mode [3]. We are uncertain of the identity of the observed state because both Λ_c^+ and Σ_c^+ can decay through these two channels. However, the Belle Collaboration [4] predicts its isospin to be zero, and the particle is predicted as a state of Λ_c.

For the Ξ_c baryon family, states belonging to the 1S and 1P wave with $J^P = \frac{1}{2}^+, \frac{1}{2}^-, \frac{3}{2}^-$ have been well established. In addition to these states, six other states are also included in the PDG [1] as shown in Table I. The spin and parity of these states, with the exception of the $\Xi_c(2970)$ state, are still unknown. The $\Xi_c(3055)^+$ and $\Xi_c(3123)^+$ states were first observed by the *BABAR* Collaboration in the $\Sigma_c(2455)^{++}K^-$ and $\Sigma_c(2520)^{++}K^-$ channel, respectively [5]. Belle confirmed the $\Xi_c(3055)^+$ state, but no signal was found for the $\Xi_c(3123)^+$ state [6]. The findings of the $\Xi_c(3080)$ state were first reported by Belle [7] and then verified by *BABAR* [5]. In 2020, LHCb observed three excited Ξ_c^0 resonances called $\Xi_c(2923)^0$, $\Xi_c(2939)^0$, and $\Xi_c(2965)^0$ in the $\Lambda_c^+K^-$ mass spectrum [8]. The $\Xi_c(2923)^0$ and $\Xi_c(2939)^0$ states were observed for the first time. This study indicates that the broad peak observed by Belle [9,10] and *BABAR* [11] for the $\Xi_c(2930)^0$ state resolves into two separate peaks for the $\Xi_c(2923)^0$ and $\Xi_c(2939)^0$ states, but the $\Xi_c(2965)^0$ state lies in the vicinity of the previously observed state $\Xi_c(2970)^0$ [5,7,12]. Thus, further study is required to establish whether or not the states $\Xi_c(2965)^0$ and $\Xi_c(2970)^0$ are equivalent. More recently in 2021, Belle reported the first experimental determination of the spin parity of $\Xi_c(2970)^+$ using the angular distribution of decay products in the chain $\Xi_c(2970)^+ \to \Xi_c(2645)^0\pi^+ \to \Xi_c^+\pi^-\pi^+$ and the ratio of the branching fraction of the two decays $\Xi_c(2970)^+ \to \Xi_c(2645)^0\pi^+/\Xi_c'^0\pi^+$ [13]. Their analysis favors $J^P = \frac{1}{2}^+$ over other possibilities with the zero spin of the light-quark degrees of freedom for $\Xi_c(2970)^+$.

For the Σ_c, Ξ_c', and Ω_c baryons, despite multiple theoretical and experimental attempts, only states belonging to the 1S wave with $J^P = \frac{1}{2}^+$ and $\frac{3}{2}^+$ have been

*Corresponding author.
raiajayk@gmail.com

TABLE I. Masses and J^P values of the experimentally observed single-charmed baryons as specified by the Particle Data Group [1]. The status is listed as poor (*), only fair (**), very likely to be certain (***), and certain (****) for their existence.

State	Mass (MeV)	J^P	Status
Λ_c^+	2286.46 ± 0.14	$\frac{1}{2}^+$	****
$\Lambda_c(2595)^+$	2592.25 ± 0.28	$\frac{1}{2}^-$	***
$\Lambda_c(2625)^+$	2628.11 ± 0.19	$\frac{3}{2}^-$	***
$\Lambda_c(2765)^+/\Sigma_c(2765)^+$	2766.6 ± 2.4	$?^?$	*
$\Lambda_c(2860)^+$	$2856.1^{+2.3}_{-6.0}$	$\frac{3}{2}^+$	***
$\Lambda_c(2880)^+$	2881.63 ± 0.24	$\frac{5}{2}^+$	***
$\Lambda_c(2940)^+$	$2939.6^{+1.3}_{-1.5}$	$\frac{3}{2}^-$	***
$\Sigma_c(2455)^{++}$	2453.97 ± 0.14	$\frac{1}{2}^+$	****
$\Sigma_c(2455)^+$	$2452.65^{+0.22}_{-0.16}$	$\frac{1}{2}^+$	****
$\Sigma_c(2455)^0$	2453.75 ± 0.14	$\frac{1}{2}^+$	****
$\Sigma_c(2520)^{++}$	$2518.41^{+0.22}_{-0.18}$	$\frac{3}{2}^+$	***
$\Sigma_c(2520)^+$	$2517.4^{+0.7}_{-0.5}$	$\frac{3}{2}^+$	***
$\Sigma_c(2520)^0$	2518.48 ± 0.20	$\frac{3}{2}^+$	***
$\Sigma_c(2800)^{++}$	2801^{+4}_{-6}	$?^?$	***
$\Sigma_c(2800)^+$	2792^{+14}_{-5}	$?^?$	***
$\Sigma_c(2800)^0$	2806^{+5}_{-7}	$?^?$	***
Ξ_c^+	2467.71 ± 0.23	$\frac{1}{2}^+$	***
Ξ_c^0	2470.44 ± 0.28	$\frac{1}{2}^+$	****
$\Xi_c'^+$	2578.2 ± 0.5	$\frac{1}{2}^+$	***
$\Xi_c'^0$	2578.7 ± 0.5	$\frac{1}{2}^+$	***
$\Xi_c(2645)^+$	2645.10 ± 0.30	$\frac{3}{2}^+$	***
$\Xi_c(2645)^0$	2646.16 ± 0.25	$\frac{3}{2}^+$	***
$\Xi_c(2790)^+$	2791.9 ± 0.5	$\frac{1}{2}^-$	***
$\Xi_c(2790)^0$	2793.9 ± 0.5	$\frac{1}{2}^-$	***
$\Xi_c(2815)^+$	2816.51 ± 0.25	$\frac{3}{2}^-$	***
$\Xi_c(2815)^0$	2819.79 ± 0.30	$\frac{3}{2}^-$	***
$\Xi_c(2923)^0$	2923.04 ± 0.35	$?^?$	**
$\Xi_c(2930)^+$	2942 ± 5	$?^?$	**
$\Xi_c(2930)^0$	2938.55 ± 0.30	$?^?$	**
$\Xi_c(2970)^+$	2964.3 ± 1.5	$\frac{1}{2}^+$	***
$\Xi_c(2970)^0$	2967.1 ± 1.7	$\frac{1}{2}^+$	***
$\Xi_c(3055)^+$	3055.9 ± 0.4	$?^?$	***
$\Xi_c(3080)^+$	3077.2 ± 0.4	$?^?$	***
$\Xi_c(3080)^0$	3079.9 ± 1.4	$?^?$	***
$\Xi_c(3123)^+$	3122.9 ± 1.3	$?^?$	*
Ω_c^0	2695.2 ± 1.7	$\frac{1}{2}^+$	***
$\Omega_c(2770)^0$	2765.9 ± 2.0	$\frac{3}{2}^+$	***
$\Omega_c(3000)^0$	3000.41 ± 0.22	$?^?$	***
$\Omega_c(3050)^0$	3050.19 ± 0.13	$?^?$	***
$\Omega_c(3065)^0$	3065.54 ± 0.26	$?^?$	***
$\Omega_c(3090)^0$	3090.1 ± 0.5	$?^?$	***
$\Omega_c(3120)^0$	3119.1 ± 1.0	$?^?$	***

discovered, and higher excited states still need to be established. So far, just one excited state of Σ_c named $\Sigma_c(2800)$ has been discovered by the Belle and *BABAR* Collaborations in the channel of $\Lambda_c^+\pi$ [14,15]. Its spin and parity are not identified yet. In 2017, LHCb declared the first observation of five narrow excited states of Ω_c^0 in the $\Xi_c^+K^-$ channel: $\Omega_c(3000)^0$, $\Omega_c(3050)^0$, $\Omega_c(3065)^0$, $\Omega_c(3090)^0$, and $\Omega_c(3120)^0$ [16]. Later, except for $\Omega_c(3120)^0$, the other four states were confirmed by the Belle Collaboration [17]. Recently, the observation of two new excited states $\Omega_c(3185)^0$ and $\Omega_c(3327)^0$ in the $\Xi_c^+K^-$ invariant-mass spectrum was revealed by the LHCb Collaboration [18]. These latest findings motivate us to identify the spin and parity of these seven states of the Ω_c^0 baryon so that they can be fitted into their mass spectrum. To achieve this, the sufficient experimental information about the Λ_c and Ξ_c baryonic states can be used to study the nature of other singly charmed baryons, such as the Σ_c, Ξ_c', and Ω_c baryons.

The spectra of singly charmed baryons have been examined by numerous theoretical models, particularly the quark model [19–28], heavy hadron chiral perturbation theory [29–31], lattice QCD [32], light cone QCD sum rules [33], QCD sum rules [34–41], Regge phenomenology [42], and the relativistic flux tube model [43–45]. In Ref. [46], the authors studied the masses of baryons containing one heavy quark in a combined expansion in $1/\mathbf{m_Q}$, $1/\mathbf{N_c}$, and SU(3) flavor symmetry breaking.

Five extremely narrow excited Ω_c baryons that were recently detected were analyzed by the authors of Ref. [47], and the possible spin assignments and the relation between the masses of different states were examined.

In our previous work [42], we employed Regge phenomenology to calculate the ground-state and excited state masses of Ω_c^0, Ω_{cc}^+, and Ω_{ccc}^{*++}. However, this model is unable to predict all possible states of a system. We aim to uncover another model that is capable of predicting the entire spectrum. In Ref. [44], the authors have analytically derived a linear Regge relation in a relativistic flux tube model for a heavy-light baryonic system. This relation is used to predict the complete spectrum of the Λ_c and Ξ_c baryons, but they exclude the study of other singly charmed baryonic systems (Σ_c, Ξ_c', and Ω_c) with a vector diquark due to the complexity of spin-dependent interactions.

In the present calculation, we apply the linear Regge relation introduced in Ref. [44] to all singly charmed baryons in the quark-diquark picture. The diquark, which is thought to be in its ground state, is assumed to excite orbitally or radially with respect to the charm quark. We incorporate spin-orbit interaction, spin-spin contact hyperfine interaction, and tensor interaction in the j-j coupling scheme to find spin-dependent splitting, and obtain the complete mass spectra of singly charmed baryons. We aim to identify the masses of fairly high orbital and radial excited states as well as assign possible quantum numbers to experimentally observed states of singly charmed baryons.

Following a brief overview of the experimental as well as theoretical progress, in Sec. II we discuss the details of the theoretical framework we use to calculate the mass spectra of singly charmed baryons. It involves the derivation of the

spin average mass formula in the relativistic flux tube model. Later, spin-dependent interactions are introduced. The parameters involved in this framework are calculated to obtain the mass spectra. In Sec. III, the obtained results are discussed to assign the spin parity to experimentally available states and to compare it with other theoretical predictions. Finally, we outline our conclusion in Sec. IV.

II. THEORETICAL FRAMEWORK

The relativistic flux tube model [48–56] has achieved phenomenological success in explaining the Regge trajectory behavior of hadrons. It is based on Nambu's idea of a dynamical gluonic string, which is responsible for the confinement of quarks within hadrons [57]. This model has been extended in a variety of ways to study mesons [58–63], baryons [44,45,64,65], as well as exotic hadrons [58,66–69]. The model is also derived from the QCD-based Wilson area law [70].

Singly charmed baryons are composed of a charm quark (c) with two light quarks (u, d, or s). According to heavy-quark symmetry, the coupling between the c quark and the light quark is predicted to be weak [71], and a strong correlation between two light quarks (u, d, or s) permits the formation of a diquark. Apart from this, the quark-diquark picture of baryons is supported by a number of theoretical arguments. A string model represents baryons as pieces of open strings connected at one common point [72]. This model predicts that a baryonic state in which three quarks are coupled to one another by three open strings that are joined at a single point in a Y shape is unstable. One of the three arms will eventually vanish, releasing its energy into the excitation modes of the other two arms. The classically stable configuration is made up of one open string connecting two quarks at the end points and one quark traveling along the string. However, in an attraction between two quarks into a $\bar{3}$ bound state, one has a configuration of one quark at one end and a diquark at the other end of a single open string. Moreover, Ref. [73] concludes that the quark-diquark structure minimizes baryon energy and is therefore preferred over the structure in which light quarks orbit around a stationary heavy quark. The author in Ref. [74] has shown that the singly heavy baryonic states with orbital angular momentum between a heavy quark and two light quarks are energetically favored compared to the states with orbital angular momentum between two light quarks. This suggests that the states where two light quarks do not excite orbitally relative to each other and behave as a bound system, i.e., a diquark, are preferred. Inspired by this theoretical evidence, we take singly charmed baryons as a diquark and charm quark pair.

In the context of the relativistic flux tube (RFT) model, a gluonic field connecting a diquark with a charm quark is proposed to lie in a straight tubelike structure called a flux tube. The color confinement is accomplished via this tube. The whole system of the charm quark, diquark, and flux tube is constantly rotating with angular speed ω around its center of mass. Along with the energy of a flux tube, this model also includes the angular momentum of a flux tube having string tension T.

The relativistic Lagrangian $\mathfrak{L}$ of the cqq baryon in the RFT model is [49]

$$\mathfrak{L} = \sum_{i=1}^{2}\left[m_i(1-r_i^2\omega^2)^{\frac{1}{2}} + T\int_0^{r_i} dr(1-r^2\omega^2)^{\frac{1}{2}}\right], \quad (1)$$

where m_1 and m_2 account for the current-quark masses of the diquark and charm quark, and r_i denotes its position from the center of mass. For simplicity, we have chosen the speed of light $c = 1$ in natural units.

We write the total orbital angular momentum L as

$$L = \frac{\partial\mathfrak{L}}{\partial\omega} = \sum_{i=1}^{2}\left[\frac{m_i v_i^2}{\omega\sqrt{1-v_i^2}} + \frac{T}{\omega^2}\int_0^{v_i}\frac{v^2dv}{(1-v)^2}\right], \quad (2)$$

where $v_i = \omega r_i$ and $v = \omega r$.

The Hamiltonian H, which is equivalent to the mass of the cqq baryon $\bar{M}$, is given by

$$H = \bar{M} = \sum_{i=1}^{2}\left[\frac{m_i}{\sqrt{1-v_i^2}} + \frac{T}{\omega}\int_0^{v_i}\frac{dv}{(1-v)^2}\right]. \quad (3)$$

We now define the effective mass of the diquark by $m_d = m_1/\sqrt{1-v_1^2}$, and that of the charm quark by $m_c = m_2/\sqrt{1-v_2^2}$, where v_1 and v_2 are the speed of the diquark and charm quark, respectively. Then, performing integration, Eqs. (2) and (3) simplify to

$$L = \frac{1}{\omega}(m_d v_1^2 + m_c v_2^2) + \frac{T}{2\omega^2}\sum_{i=1}^{2}\left(\sin^{-1}v_i - v_i\sqrt{1-v_i^2}\right) \quad (4)$$

and

$$\bar{M} = m_d + m_c + \frac{T}{\omega}\sum_{i=1}^{2}\sin^{-1}v_i. \quad (5)$$

The boundary condition at the end of the flux tube with the charm quark gives

$$\frac{T}{\omega} = \frac{m_c v_2}{\sqrt{1-v_2^2}} = m_c v_2\left[1 + \frac{v_2^2}{2} + \frac{3v_2^4}{8} + \cdots\right] \simeq m_c v_2, \quad (6)$$

where higher order terms of v_2 are neglected.

For singly charmed baryons, $m_d \ll m_c$. With this limit of a very small mass of the diquark, we take the speed-of-light diquark $v_1 \approx 1$ for approximation. Expanding Eqs. (4) and

(5) in terms of v_2 up to second order and using Eq. (6), the mass relation can be obtained as [44]

$$(\bar{M} - m_c)^2 = \frac{\sigma}{2}L + (m_d + m_c v_2^2), \tag{7}$$

where $\sigma = 2\pi T$. This gives a Regge-like relation between the mass and angular momentum. The method used in this study can be thought of as a semiclassical approximation of the quantized theory of strings, as L is taken as the angular momentum quantum number. Despite the fact that we did not account for the quantum correction, the obtained Regge relation shows the basic features predicted by a fully quantum mechanical approach [52,53,56], such as the linear nature of the Regge trajectory and nonzero intercept for the $L = 0$ state in the $(L, (\bar{M} - m_c)^2)$ plane.

Now, the distance between a heavy and light component of the baryon can be given as

$$r = \frac{v_1 + v_2}{\omega} = (v_1 + v_2)\sqrt{\frac{8L}{\sigma}}, \tag{8}$$

where the relation between the angular speed of the rotation of flux tube and orbital angular momentum $\omega = \sqrt{\sigma/8L}$ is obtained by combining Eqs. (4) and (7).

In Refs. [52,53,56], the RFT model is solved for heavy-light mesons with a quantum mechanical approach, which gives a nearly straight leading Regge trajectory in the $(L, (\bar{M} - m_c)^2)$ plane, which is followed by nearly parallel and equally spaced daughter trajectories. In our model, the singly charmed baryons are pictured as a two-body system with one heavy quark, the same as heavy-light mesons, where one quark is heavy. So, for singly charmed baryons with a two-body picture, we will also get nearly straight, parallel, and equally spaced Regge trajectories. In light of these quantum mechanical studies that show Regge trajectories in the $(L, (\bar{M} - m_c)^2)$ plane with various values of n (radial excitation quantum number) to be parallel to one another, we extend our semiclassical relation (7) and (8) for radially excited states by replacing L with $(\lambda n + L)$ as

$$(\bar{M} - m_c)^2 = \frac{\sigma}{2}[\lambda n_r + L] + (m_d + m_c v_2^2) \tag{9}$$

and

$$r = (v_1 + v_2)\sqrt{\frac{8[\lambda n_r + L]}{\sigma}}, \tag{10}$$

where λ is an unknown parameter that we extracted using experimental data. Here, $n_r = n - 1$ where n represents the principal quantum number of the baryon state.

The RFT model considers the quarks to be spinless; hence, we now incorporate spin-dependent interactions to get the complete mass spectra. The resulting mass takes the form

$$M = \bar{M} + \Delta M, \tag{11}$$

where the spin average mass $\bar{M}$ can be obtained from Eq. (9), and the contribution to mass from spin-dependent interaction is given by

$$\Delta M = H_{so} + H_t + H_{ss}. \tag{12}$$

Here, the first term is spin-orbit interaction, with the form

$$\begin{aligned} H_{so} &= \left[\left(\frac{2\alpha}{3r^3} - \frac{b'}{2r}\right)\frac{1}{m_d^2} + \frac{4\alpha}{3r^3}\frac{1}{m_c m_d}\right]\mathbf{L}.\mathbf{S_d} \\ &\quad + \left[\left(\frac{2\alpha}{3r^3} - \frac{b'}{2r}\right)\frac{1}{m_c^2} + \frac{4\alpha}{3r^3}\frac{1}{m_c m_d}\right]\mathbf{L}.\mathbf{S_c} \\ &= a_1\mathbf{L}.\mathbf{S_d} + a_2\mathbf{L}.\mathbf{S_c}, \end{aligned} \tag{13}$$

which results from the short-range one-gluon exchange contribution and the long-range Thomas-precession term [75]. The second spin-dependent interaction

$$\begin{aligned} H_t &= \frac{4\alpha}{3r^3}\frac{1}{m_c m_d}\left[\frac{3(\mathbf{S_d}.\mathbf{r})(\mathbf{S_c}.\mathbf{r})}{r^2} - \mathbf{S_d}.\mathbf{S_c}\right] \\ &= b\hat{B} \end{aligned} \tag{14}$$

arises from magnetic-dipole-magnetic-dipole color hyperfine interaction and is a tensor term. Here, $\hat{B} = 3(\mathbf{S_d}.\mathbf{r})(\mathbf{S_c}.\mathbf{r})/r^2 - \mathbf{S_d}.\mathbf{S_c}$. The last term

$$H_{ss} = \frac{32\alpha\sigma_0^3}{9\sqrt{\pi}m_c m_d}e^{-\sigma_0^2 r^2}\mathbf{S_d}.\mathbf{S_c} = c\mathbf{S_d}.\mathbf{S_c} \tag{15}$$

is the spin-spin contact hyperfine interaction. The parameters b' and σ_0 can be fixed using experimental data. α is the coupling constant. $\mathbf{S_c}$ and $\mathbf{S_d}$ denote the spin of the charm quark and diquark, respectively.

As per Pauli's exclusion principle, the total symmetry of a diquark under an exchange of two quarks is antisymmetric. A diquark has a symmetric spatial state and an antisymmetric color state [76]. The flavor and spin states of a diquark can either be symmetric or antisymmetric, such that $|\text{flavor}\rangle \times |\text{spin}\rangle$ is symmetric. As shown in Fig. 1, the

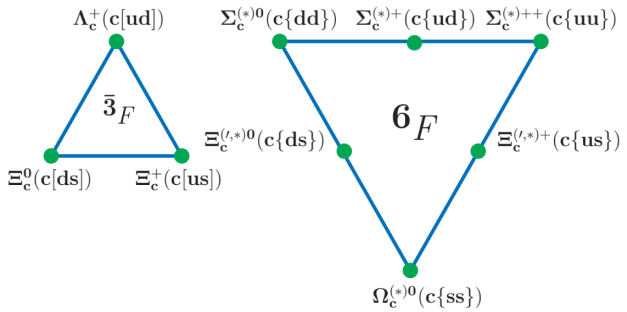

FIG. 1. Antitriplet ($\bar{3}_F$) and sextet (6_F) representation of singly charmed baryons.

flavor symmetries of light quarks organize singly charmed baryons into two groups: an antisymmetric antitriplet ($\bar{3}_F$) and symmetric sextet (6_F), as $3 \otimes 3 = 6_F \oplus \bar{3}_F$. The symmetric flavor state of a diquark requires a symmetric spin state, whereas the antisymmetric flavor state of a diquark requires an antisymmetric spin state. As a result, baryons that belong to the antitriplet (Λ_c and Ξ_c baryons) have a spin-zero diquark (also known as a scalar diquark $[q_1, q_2]$), whereas those that belong to the sextet (Σ_c, Ξ_c', and Ω_c baryons) have a spin-one diquark (also known as a vector diquark $\{q_1, q_2\}$). Here, q_1 and q_2 are one of a u, d, or s quark.

There are two ways by which $\mathbf{S_c}$, $\mathbf{S_d}$, and $\mathbf{L}$ can couple to give total angular momentum $\mathbf{J}$. First is the L-S coupling scheme in which the spin of diquark $\mathbf{S_d}$ first couples with the spin of charm quark $\mathbf{S_c}$ to form $\mathbf{S}$, and later $\mathbf{S}$ couples with $\mathbf{L}$ to give $\mathbf{J}$. The second one is the j-j coupling scheme, which is the dominant one in the heavy-quark limit, where a spin of diquark $\mathbf{S_d}$ first couples with $\mathbf{L}$ and results in total angular momentum of diquark $\mathbf{j}$, and then $\mathbf{j}$ couples with a spin of charm quark $\mathbf{S_c}$ to give $\mathbf{J}$. Since $m_c \gg m_d$ for single-charmed baryons, we assume that heavy-quark symmetry is followed. This allows us to refer to baryonic states as a j-j coupling state $|J, j\rangle$, where both $\mathbf{j}$ and $\mathbf{J}$ are conserved.

For the Λ_c and Ξ_c baryons, with a scalar diquark ($S_d = 0$), both L-S and j-j coupling schemes give identical states. Spin interactions are much simpler, as only the second term of the spin-orbit interaction survives, and the tensor, as well as the spin-spin contact hyperfine interactions, become zero. The expectation value of $\mathbf{L}.\mathbf{S_c}$ in any coupling scheme for Λ_c and Σ_c is given by

$$\langle \mathbf{L}.\mathbf{S_c} \rangle = \frac{1}{2}[J(J+1) - L(L+1) - S_c(S_c+1)]. \quad (16)$$

The spin interactions for the Σ_c, Ξ_c', and Ω_c baryons, with vector diquark ($S_d = 1$), are more complex than those for the Λ_c and Ξ_c baryons. A detailed calculation of the mass-splitting operators in the j-j coupling scheme that is involved in spin-dependent interactions is shown in the Appendix and the results are listed in Table II.

TABLE II. Matrix elements for spin interaction for different states for a singly heavy baryon with a vector diquark.

(L, J, j)	$\langle S_d.L \rangle$	$\langle S_c.L \rangle$	$\langle \hat{B} \rangle$	$\langle S_d.S_c \rangle$
$(S, 1/2, 1)$	0	0	0	−1
$(S, 3/2, 1)$	0	0	0	1/2
$(P, 1/2, 0)$	−2	0	0	0
$(P, 1/2, 1)$	−1	−1/2	−1	−1/2
$(P, 3/2, 1)$	−1	1/4	1/2	1/4
$(P, 3/2, 2)$	1	−3/4	3/10	−3/4
$(P, 5/2, 2)$	1	1/2	−1/5	1/2
$(D, 1/2, 1)$	−3	−3/2	−1	1/2
$(D, 3/2, 1)$	−3	3/4	1/2	−1/4
$(D, 3/2, 2)$	−1	−5/4	−1/2	−1/4
$(D, 5/2, 2)$	2	−4/3	8/21	−2/3
$(D, 5/2, 3)$	−1	5/6	1/3	1/6
$(D, 7/2, 3)$	2	1	−2/7	1/2

A. Mass spectra of the Λ_c and Ξ_c baryons

Experimental research has revealed a wide variety of Λ_c baryonic states. This gives us context for fixing unidentified parameters in our model. The parameters m_c, v_1, v_2, λ, α, and b' can be fixed from experimentally available states of Λ_c and are taken as common parameters for all singly charmed baryons to ensure consistency in the model. The remaining parameters, such as the diquark mass m_d, string tension σ, and σ_0, depend on the system under consideration. The ultrarelativistic nature of the light diquark leads us to believe that $v_1 \approx 1$. The spin-averaged mass of the nL wave is [77]

$$\bar{M}_{nL} = \frac{\sum_J (2J+1) M_J}{\sum_J (2J+1)}, \quad (17)$$

where the summation is taken over all possible states of the nL wave with spin J and mass M_J. The spin-average mass of the $1S$, $1P$, and $1D$ states is calculated using the corresponding experimental states of the Λ_c^+ baryons, which is then utilized to determine the parameters $m_c = 1.448$ GeV, $\sigma_{\Lambda_c} = 1.323$ GeV^2, and $m_{d_{[u,d]}} + m_c v_2^2 = 0.838$ GeV. We fix the velocity charm quark equal to 0.48 by comparing the mass of charm quark m_c to its current-quark mass 1.27 ± 0.025 GeV [1]. This yields $m_{d_{[u,d]}} = 0.503$ GeV. The experimental mass of the $\Lambda_c(2765)^+$ state and the predicted mass of the $|2S, 1/2^+\rangle$ state from the relativistic quark model in Ref. [23] are highly comparable, so it makes sense to accept this conclusion and adapt it to extract $\lambda = 1.565$. For the Λ_c baryon, H_t and H_{ss} becomes zero. Thus, we fix $\alpha = 0.426$ and $b' = -0.076$ GeV^2 in Eq. (13) using the splitting in the $1P$ and $1D$ wave. Utilizing the above parameters, the mass spectra of Λ_c baryon is extracted, which is shown in Table III with comparisons with other Refs. [20,23,25,26,44]. For the Ξ_c baryons, with the spin-averaged masses of $1S$ and $1P$, which we calculate using experimentally detected states, we extract the mass of the diquark $m_{d_{[d,s]}} = 0.687$ GeV and $\sigma_{\Xi_c} = 1.625$ GeV^2. With these parameters, we determine the masses of the Ξ_c baryonic states, which are given in Table IV. Our predicted mass for the first radially excited state $|2S, 1/2^+\rangle$ of the Ξ_c baryon is 2970.5 MeV, which is only 3.4 MeV different from the experimentally detected mass of 2967.10 MeV. This confirms that the extracted value of $\lambda = 1.565$ from the experimental data of the Λ_c baryon is reliable.

B. Mass spectra of the Σ_c, Ξ_c', and Ω_c baryons

Using an experimental spin-average mass of the $1S$ wave of these three systems, we first find a mass of

TABLE III. Masses of the Λ_c^+ baryon (in MeV).

(n, L, J, j)	States $\|nL, J^P\rangle$	Present	PDG [1]	[23]	[26]	[44]	[25]	[20]
(1, 0, 1/2, 0)	$\|1S, 1/2^+\rangle$	2286.5	2286.46(0.14)	2286	2286	2286	2286	2268
(2, 0, 1/2, 0)	$\|2S, 1/2^+\rangle$	2766.6	2766.6(0.24)	2769	2772	2766	2699	2791
(3, 0, 1/2, 0)	$\|3S, 1/2^+\rangle$	3113.6		3130	3116	3112	3053	
(4, 0, 1/2, 0)	$\|4S, 1/2^+\rangle$	3399.9		3437		3397	3398	
(1, 1, 1/2, 1)	$\|1P, 1/2^-\rangle$	2592.3	2592.25(0.28)	2598	2614	2591	2629	2625
(1, 1, 3/2, 1)	$\|1P, 3/2^-\rangle$	2628.1	2628.11(0.19)	2627	2639	2629	2612	2636
(2, 1, 1/2, 1)	$\|2P, 1/2^-\rangle$	2989.6	$2939.6^{+1.3}_{-1.5}$	2983	2980	2989	2962	2816
(2, 1, 3/2, 1)	$\|2P, 3/2^-\rangle$	3001.1	$2939.6^{+1.3}_{-1.5}$	3005	3004	3000	2944	2830
(3, 1, 1/2, 1)	$\|3P, 1/2^-\rangle$	3296.9		3303		3296	3295	
(3, 1, 3/2, 1)	$\|3P, 3/2^-\rangle$	3303.9		3322		3301	3276	
(4, 1, 1/2, 1)	$\|4P, 1/2^-\rangle$	3559.1		3588			3630	
(4, 1, 3/2, 1)	$\|4P, 3/2^-\rangle$	3564.3		3606			3610	
(1, 2, 3/2, 2)	$\|1D, 3/2^+\rangle$	2856.1	$2856.1^{+2.3}_{-6.0}$	2874	2843	2857	2873	2887
(1, 2, 5/2, 2)	$\|1D, 5/2^+\rangle$	2881.6	2881.63(0.24)	2880	2851	2879	2849	2887
(2, 2, 3/2, 2)	$\|2D, 3/2^+\rangle$	3189.6		3189		3188	3207	3073
(2, 2, 5/2, 2)	$\|2D, 5/2^+\rangle$	3203.2		3209		3198	3179	
(3, 2, 3/2, 2)	$\|3D, 3/2^+\rangle$	3466.4		3480				
(3, 2, 5/2, 2)	$\|3D, 5/2^+\rangle$	3476.0		3500				
(4, 2, 3/2, 2)	$\|4D, 3/2^+\rangle$	3709.1		3747				
(4, 2, 5/2, 2)	$\|4D, 5/2^+\rangle$	3716.6		3767				
(1, 3, 5/2, 3)	$\|1F, 5/2^-\rangle$	3074.4		3097		3075	3116	2872
(1, 3, 7/2, 3)	$\|1F, 7/2^-\rangle$	3097.2		3078		3092	3079	
(2, 3, 5/2, 3)	$\|2F, 5/2^-\rangle$	3369.0		3375				
(2, 3, 7/2, 3)	$\|2F, 7/2^-\rangle$	3384.0		3393				
(3, 3, 5/2, 3)	$\|3F, 5/2^-\rangle$	3622.9		3646				
(3, 3, 7/2, 3)	$\|3F, 7/2^-\rangle$	3634.3		3667				
(1, 4, 7/2, 4)	$\|1G, 7/2^+\rangle$	3265.9		3270		3267		
(1, 4, 9/2, 4)	$\|1G, 9/2^+\rangle$	3287.8		3284		3280		
(2, 4, 7/2, 4)	$\|2G, 7/2^+\rangle$	3533.1		3546				
(2, 4, 9/2, 4)	$\|2G, 9/2^+\rangle$	3549.1		3564				
(1, 5, 9/2, 5)	$\|1H, 9/2^-\rangle$	3438.9		3444				
(1, 5, 11/2, 5)	$\|1H, 11/2^-\rangle$	3460.4		3460				

diquark $m_{d_{\{u,u\}}} = 0.714$ GeV, $m_{d_{\{d,s\}}} = 0.841$ GeV, and $m_{d_{\{s,s\}}} = 0.959$ GeV. In spin-dependent interactions for an S wave, only a spin-spin contact hyperfine interaction contributes. Thus, the parameter involved in this interaction, σ_0, is calculated using a splitting in the $1S$ wave as the $\sigma_{0_{\Sigma_c}} = 0.373$ GeV, $\sigma_{0_{\Xi_c'}} = 0.400$ GeV, and $\sigma_{0_{\Omega_c}} = 0.425$ GeV systems, respectively. We take a spin-average mass of the $2S$ wave of Σ_c as input from Ref. [23] to fix $\lambda = 1.295$ for these systems.

For the Σ_c, Ξ_c', and Ω_c baryons, states belonging to the $1P$ wave have not yet been established experimentally, so we cannot find the value of σ directly from experimental data, as we did for the Λ_c and Ξ_c baryons. To find the string tension for the Σ_c and Ξ_c' baryons, the authors in Ref. [45] rely on the assumption that the orbital trajectory of the Λ_c and Σ_c baryons as well as the Ξ_c and Ξ_c' baryons is parallel, leading to similar string tensions between them. But as shown in Table V, this assumption is not supported by the analysis of mass spectra of singly charmed baryons in the relativistic quark potential model [23,78]. In this model, as the diquark's mass increases, we see that the Regge slope in the (L, $(\bar{M} - m_c)^2$) plane, or string tension, also increases.

Within the singly charmed baryonic family, all systems have an identical heavy component, which is a charm quark, but the light diquark has different spin (0 or 1) or quark combinations with which the mass of the diquark varies. Hence, the string tension of these systems should be a functional of the mass of the diquark only. For simplicity, we assume that string tension is proportional to some power q of the mass of the diquarks,

$$\sigma \propto m_d^q. \tag{18}$$

A recent study by Song *et al.* on doubly heavy baryons uses a similar type of power-law assumption for the string tensions of heavy-light hadrons [65]. Taking the ratio of the string tensions of Ξ_c and Λ_c, we obtain

$$\frac{\sigma_{\Xi_c}}{\sigma_{\Lambda_c}} = \left(\frac{m_{d_{[d,s]}}}{m_{d_{[u,d]}}}\right)^q. \tag{19}$$

By applying the above relation, we first fix $q = 0.661$, and then we find σ for the Σ_c, Ξ_c', and Ω_c baryons using the ratios

$$\frac{\sigma_{\Sigma_c}}{\sigma_{\Lambda_c}} = \left(\frac{m_{d_{\{u,u\}}}}{m_{d_{[u,d]}}}\right)^q, \tag{20}$$

$$\frac{\sigma_{\Xi_c'}}{\sigma_{\Lambda_c}} = \left(\frac{m_{d_{\{d,s\}}}}{m_{d_{[u,d]}}}\right)^q, \tag{21}$$

and

$$\frac{\sigma_{\Omega_c}}{\sigma_{\Lambda_c}} = \left(\frac{m_{d_{\{s,s\}}}}{m_{d_{[u,d]}}}\right)^q \tag{22}$$

as $\sigma_{\Sigma_c} = 1.666\ \text{GeV}^2$, $\sigma_{\Xi_c'} = 1.856\ \text{GeV}^2$, and $\sigma_{\Omega_c} = 2.026\ \text{GeV}^2$. Other parameters m_c, v_1, v_2, α, and b fixed for Λ_c and Ξ_c are taken as the inputs. These parameters are used to determine the masses of the Σ_c, Ξ_c', and Ω_c baryonic states, which are given in Tables VI–VIII. From the assumption that string tension depends on the qth power of the mass of the diquark, we have successfully reproduced experimentally detected states of the Σ_c, Ξ_c', and Ω_c baryons.

III. RESULTS AND DISCUSSION

This section discusses our results for the mass spectra of single-charmed baryons. The ground-state and excited state masses for the Λ_c, Ξ_c, Σ_c, Ξ_c', and Ω_c baryons are shown in Tables III–VIII, respectively. These tables provide the baryon quantum numbers (n, L, J, j) and corresponding baryonic states $|nL, J^P\rangle$ in the first two columns, together with our predicted masses, experimental masses, and prediction from other models in the remaining columns. Further, we have constructed the Regge trajectories for these baryons in the (J, M^2) plane with natural and unnatural parity states as shown in Figs. 2–9. We have found that the available experimental masses nicely fit. Also, it can be seen that these trajectories are almost linear, parallel, and equidistant. We are now attempting to relate the experimentally observed states of singly charmed baryons to our model predictions for the following baryons:

(1) Λ_c baryon: Our results for the mass spectra of the Λ_c baryon are presented in Table III. The $1S$, $1P$, and $1D$ states of the Λ_c baryon are already well established in an experiment. The masses of these states are well reproduced in our model. The PDG lists the highest state $\Lambda_c(2940)$ baryon with $2939.6^{+1.3}_{-1.5}$ MeV mass. Its favored spin parity in PDG is $J^P = \frac{3}{2}^-$, but it is not certain. The measured mass of the $\Lambda_c(2940)$ baryon is near our predicted masses for the $|2P, 1/2^-\rangle$ and $|2P, 3/2^-\rangle$ states with a slightly higher mass difference of 50 and 61.5 MeV, respectively. The predictions in Refs. [23,78,79] also show nearly the same mass difference from the experimental value. Thus, the $\Lambda_c(2940)$ can be assigned to one of the $2P$ states with $J^P = \frac{1}{2}^-$ or $J^P = \frac{3}{2}^-$.

(2) Ξ_c and Ξ_c' baryon: The predicted masses of Ξ_c and Ξ_c' baryons are given in Tables IV and VII, respectively. Experimentally, it is not possible to distinguish between the excited states of the Ξ_c and Ξ_c' baryons. Hence, PDG simply lists them as Ξ_c. As shown in Table I, many excited states of the Ξ_c and Ξ_c' baryons have been reported experimentally. Because of the small mass difference between these states, it is highly challenging to assign spin parity to them. Recently, the Belle Collaboration concluded that the $\Xi_c(2970)$ state belongs to the $J^P = \frac{1}{2}^+$ state with the zero spin of the light-quark degrees of freedom [13]. Our theoretical prediction for the $|2S, 1/2^+\rangle$ state of the Ξ_c baryon with a scalar diquark differs only by 3.4 MeV from the measured mass of the $\Xi_c(2970)$ state. As a result, our calculation agrees very well with Belle's $J^P = \frac{1}{2}^+$ assignment for the $\Xi_c(2970)$ state. Moreover, the LHCb Collaboration discovered the $\Xi_c(2965)^0$ state [8], which lies very close to the previously observed $\Xi_c(2970)$ state. More research is needed to determine whether $\Xi_c(2965)^0$ is the isospin partner of $\Xi_c(2970)^+$ or a distinct state of the Ξ_c baryon. Our predictions for the masses of the $2S$ states with $J^P = \frac{1}{2}^+$ and $\frac{3}{2}^+$ of the Ξ_c' baryon differ from the experimental mass of $\Xi_c(3055)$ by only 6.6 and 3 MeV, respectively, as shown in Table VII. The mass of the $\Xi_c(3055)$ state is also very close to our prediction for the Ξ_c baryon's second orbital excitation $(1D)$ with $J^P = \frac{3}{2}^+$. As a result, $\Xi_c(3055)$ can be interpreted as one of the radial excitations $(2S)$ of the Ξ_c' baryon with $J^P = \frac{1}{2}^+$ or $\frac{3}{2}^+$, or it may belong to the $1D$ state of the Ξ_c baryon with $J^P = \frac{3}{2}^+$. Only through future experiments will it be possible to identify the appropriate assignment. The $\Xi_c(3080)$ with mass 3079.9 MeV is listed by the PDG with a status of three stars. This mass is only 13.4 MeV larger than the model prediction for the $1D$ state of the Ξ_c baryon with $J^P = \frac{5}{2}^+$. So, $\Xi_c(3080)$ is a good candidate for second orbital excitation $(1D)$ of the Ξ_c baryon and we assign $J^P = \frac{5}{2}^+$ to this state. The $\Xi_c(3123)$ was first observed by the *BABAR* Collaboration [5]. The evidence for this state is quite weak, as the Belle Collaboration [6] did not find any signal for this state, and the PDG lists it with a status of one star only. In our work, the $|1D, 5/2^+\rangle$ state of

TABLE IV. Masses of the Ξ_c baryon (in MeV).

(n, L, J, j)	States $\|nL, J^P\rangle$	Present	PDG [1]	[23]	[26]	[44]	[20]
(1, 0, 1/2, 0)	$\|1S, 1/2^+\rangle$	2470.4	2470.44(0.28)	2476	2470	2467	2466
(2, 0, 1/2, 0)	$\|2S, 1/2^+\rangle$	2970.5	2967.10(1.7)	2959	2940	2959	2924
(3, 0, 1/2, 0)	$\|3S, 1/2^+\rangle$	3342.8		3323	3265	3325	
(4, 0, 1/2, 0)	$\|4S, 1/2^+\rangle$	3653.1		3632		3629	
(1, 1, 1/2, 1)	$\|1P, 1/2^-\rangle$	2785.7	2793.90(0.5)	2792	2793	2779	2773
(1, 1, 3/2, 1)	$\|1P, 3/2^-\rangle$	2823.9	2819.79(0.3)	2819	2820	2814	2783
(2, 1, 1/2, 1)	$\|2P, 1/2^-\rangle$	3209.1		3179	3140	3195	
(2, 1, 3/2, 1)	$\|2P, 3/2^-\rangle$	3221.5		3201	3164	3204	
(3, 1, 1/2, 1)	$\|3P, 1/2^-\rangle$	3541.2		3500		3521	
(3, 1, 3/2, 1)	$\|3P, 3/2^-\rangle$	3548.9		3519		3525	
(4, 1, 1/2, 1)	$\|4P, 1/2^-\rangle$	3826.5		3785			
(4, 1, 3/2, 1)	$\|4P, 3/2^-\rangle$	3832.2		3804			
(1, 2, 3/2, 2)	$\|1D, 3/2^+\rangle$	3065.9	3055.9(0.4)	3059	3033	3055	3012
(1, 2, 5/2, 2)	$\|1D, 5/2^+\rangle$	3093.3	3079.9(1.4)	3076	3040	3076	3004
(2, 2, 3/2, 2)	$\|2D, 3/2^+\rangle$	3425.0		3388		3407	
(2, 2, 5/2, 2)	$\|2D, 5/2^+\rangle$	3439.7		3407		3416	
(3, 2, 3/2, 2)	$\|3D, 3/2^+\rangle$	3725.6		3678			
(3, 2, 5/2, 2)	$\|3D, 5/2^+\rangle$	3735.9		3699			
(4, 2, 3/2, 2)	$\|4D, 3/2^+\rangle$	3990.2		3945			
(4, 2, 5/2, 2)	$\|4D, 5/2^+\rangle$	3998.4		3965			
(1, 3, 5/2, 3)	$\|1F, 5/2^-\rangle$	3300.5		3278		3286	
(1, 3, 7/2, 3)	$\|1F, 7/2^-\rangle$	3325.0		3292		3302	
(2, 3, 5/2, 3)	$\|2F, 5/2^-\rangle$	3619.6		3575			
(2, 3, 7/2, 3)	$\|2F, 7/2^-\rangle$	3635.8		3592			
(3, 3, 5/2, 3)	$\|3F, 5/2^-\rangle$	3896.2		3845			
(3, 3, 7/2, 3)	$\|3F, 7/2^-\rangle$	3908.6		3865			
(1, 4, 7/2, 4)	$\|1G, 7/2^+\rangle$	3507.7		3469		3490	
(1, 4, 9/2, 4)	$\|1G, 9/2^+\rangle$	3531.3		3483		3503	
(2, 4, 7/2, 4)	$\|2G, 7/2^+\rangle$	3798.2		3745			
(2, 4, 9/2, 4)	$\|2G, 9/2^+\rangle$	3815.5		3763			
(1, 5, 9/2, 5)	$\|1H, 9/2^-\rangle$	3695.6		3643			
(1, 5, 11/2, 5)	$\|1H, 11/2^-\rangle$	3719.0		3658			

the Ξ_c baryon and the $|1D, 1/2^+\rangle$ state of the Ξ_c' baryon lies at 3093.3 and 3157.1 MeV, respectively. The masses of these two states lie relatively closer to the measured mass of $\Xi_c(3123)$ with a deviation of 29.6 and 34.2 MeV, respectively. Because the $|1D, 5/2^+\rangle$ state of the Ξ_c baryon is assigned to the $\Xi_c(3080)$ in our work, the only possibility for the $\Xi_c(3123)$ is that it is the $1D$ state of the Ξ_c' baryon with $J^P = \frac{1}{2}^+$. Finally, the $\Xi_c(2923)$ and $\Xi_c(2938)$ states are interpreted as the first orbital $(1P)$ excitations of the Ξ_c' baryon with $J^P = \frac{1}{2}^-$ and $\frac{3}{2}^-$, respectively.

TABLE V. In the relativistic quark model, the mass of the diquark and the slope of the Regge trajectory in the (L, $(\bar{M} - m_c)^2$) plane [23,78]. This data show that within a singly charmed baryonic family, the slope of the Regge trajectory in the (L, $(\bar{M} - m_c)^2$) plane increases along with the mass of the diquark.

Baryon	m_d (GeV)	Regge slope (GeV^{-2})
Λ_c	0.710	0.615
Σ_c	0.909	0.683
Ξ_c	0.948	0.711
Ξ_c'	1.069	0.752
Ω_c	1.203	0.812

(3) Σ_c baryon: The masses of the Σ_c baryonic states as predicted by the RFT model are summarized in Table VI with the available experimental masses and comparison with other theoretical models. So far, only one excited state of the Σ_c baryon, namely, $\Sigma_c(2800)$, has been discovered with mass 2801^{+4}_{-6} MeV. Its spin and parity have not been identified yet. Our predicted mass of 2800.1 MeV for the $|1P, 3/2^-\rangle$ state is in excellent agreement with the experimental mass. Thus, $\Sigma_c(2800)$ is a good candidate for the 1P state with $J^P = \frac{3}{2}^-$. Apart from this state, many other states belonging to the $1P$ wave in the vicinity of the $\Sigma_c(2800)$ state are predicted. These are the states most likely to be detected first in the experiment. This prediction will definitely be

TABLE VI. Masses of the Σ_c baryon (in MeV).

(n, L, J, j)	States $\|nL, J^P\rangle$	Present	PDG [1]	[23]	[26]	[25]	[20]
(1, 0, 1/2, 1)	$\|1S, 1/2^+\rangle$	2454.0	2453.97(0.14)	2443	2456	2454	2455
(1, 0, 3/2, 1)	$\|1S, 3/2^+\rangle$	2518.4	$2518.41^{+0.22}_{-0.18}$	2519	2515	2530	2519
(2, 0, 1/2, 1)	$\|2S, 1/2^+\rangle$	2917.9		2901	2850	3016	2958
(2, 0, 3/2, 1)	$\|2S, 3/2^+\rangle$	2927.6		2936	2876	3069	2995
(3, 0, 1/2, 1)	$\|3S, 1/2^+\rangle$	3252.3		3271	3091	3492	
(3, 0, 3/2, 1)	$\|3S, 3/2^+\rangle$	3253.7		3293	3109	3525	
(1, 1, 1/2, 0)	$\|1P, 1/2^-\rangle$	2727.8		2713	2702	2890	2748
(1, 1, 1/2, 1)	$\|1P, 1/2^-\rangle$	2749.3		2799	2765	2906	2768
(1, 1, 3/2, 1)	$\|1P, 3/2^-\rangle$	2800.1	2801^{+4}_{-6}	2773	2785	2860	2763
(1, 1, 3/2, 2)	$\|1P, 3/2^-\rangle$	2872.1		2798	2798	2875	2776
(1, 1, 5/2, 2)	$\|1P, 5/2^-\rangle$	2908.5		2789	2790	2835	2790
(2, 1, 1/2, 0)	$\|2P, 1/2^-\rangle$	3134.8		3125	2971	3352	
(2, 1, 1/2, 1)	$\|2P, 1/2^-\rangle$	3149.2		3172	3018	3369	
(2, 1, 3/2, 1)	$\|2P, 3/2^-\rangle$	3164.3		3151	3036	3318	
(2, 1, 3/2, 2)	$\|2P, 3/2^-\rangle$	3201.5		3172	3044	3335	
(2, 1, 5/2, 2)	$\|2P, 5/2^-\rangle$	3212.8		3161	3040	3290	

helpful for future experiments to detect these unobserved states.

(4) Ω_c baryon: Recently, five narrow excited states of the Ω_c baryon, namely, Ω_c^0, $\Omega_c(3050)^0$, $\Omega_c(3065)^0$, $\Omega_c(3090)^0$, and $\Omega_c(3120)^0$, have been detected, the spin parity of which is unknown. Our predicted masses for the Ω_c states, as shown in Table VIII, help to determine the possible quantum numbers of these experimentally detected states. From the RFT model, we propose that all of these newly observed states of the Ω_c^0 baryon belong to the $1P$ wave. The experimentally measured mass of the $\Omega_c(3000)^0$ state, 3000.41 MeV, is very close to the model prediction of 3003.2 MeV for the $|1P, 1/2^-\rangle_{j=0}$ state. Hence, we assign $J^P = \frac{1}{2}^-$ for $\Omega_c(3000)^0$. The measured mass of the $\Omega_c(3065)^0$ state is only

TABLE VII. Masses of the Ξ_c' baryon (in MeV).

(n, L, J, j)	States $\|nL, J^P\rangle$	Present	PDG [1]	[23]	[26]	[20]
(1, 0, 1/2, 1)	$\|1S, 1/2^+\rangle$	2578.7	2578.70(0.5)	2579	2579	2594
(1, 0, 3/2, 1)	$\|1S, 3/2^+\rangle$	2646.2	2646.16(0.25)	2649	2649	2649
(2, 0, 1/2, 1)	$\|2S, 1/2^+\rangle$	3049.3	3055.9(0.4)	2983	2977	
(2, 0, 3/2, 1)	$\|2S, 3/2^+\rangle$	3058.9	3055.9(0.4)	3026	3007	
(3, 0, 1/2, 1)	$\|3S, 1/2^+\rangle$	3393.1		3377	3215	
(3, 0, 3/2, 1)	$\|3S, 3/2^+\rangle$	3394.5		3396	3236	
(1, 1, 1/2, 0)	$\|1P, 1/2^-\rangle$	2873.3		2854	2839	2855
(1, 1, 1/2, 1)	$\|1P, 1/2^-\rangle$	2886.4	2923.04(0.35)	2936	2900	
(1, 1, 3/2, 1)	$\|1P, 3/2^-\rangle$	2937.9	2938(0.3)	2912	2921	2866
(1, 1, 3/2, 2)	$\|1P, 3/2^-\rangle$	2992.9		2935	2932	
(1, 1, 5/2, 2)	$\|1P, 5/2^-\rangle$	3030.5		2929	2927	2989
(2, 1, 1/2, 0)	$\|2P, 1/2^-\rangle$	3282.0		3267	3094	
(2, 1, 1/2, 1)	$\|2P, 1/2^-\rangle$	3291.9		3313	3144	
(2, 1, 3/2, 1)	$\|2P, 3/2^-\rangle$	3307.3		3293	3172	
(2, 1, 3/2, 2)	$\|2P, 3/2^-\rangle$	3335.4		3311	3165	
(2, 1, 5/2, 2)	$\|2P, 5/2^-\rangle$	3347.2		3303	3170	
(1, 2, 1/2, 1)	$\|1D, 1/2^+\rangle$	3157.1	3122.9	3163	3075	
(1, 2, 3/2, 1)	$\|1D, 3/2^+\rangle$	3189.8		3160	3089	
(1, 2, 3/2, 2)	$\|1D, 3/2^+\rangle$	3207.1		3167	3081	
(1, 2, 5/2, 3)	$\|1D, 5/2^+\rangle$	3236.6		3153	3091	
(1, 2, 5/2, 2)	$\|1D, 5/2^+\rangle$	3279.0		3166	3077	
(1, 2, 7/2, 3)	$\|1D, 7/2^+\rangle$	3304.6		3147	3078	

TABLE VIII. Masses of the Ω_c baryon (in MeV).

(n, L, J, j)	States $\|nL, J^P\rangle$	Present	PDG [1]	[23]	[42]	[20]	[25]
(1, 0, 1/2, 1)	$\|1S, 1/2^+\rangle$	2695.2	2695.2(1.7)	2698	2702	2718	2695
(1, 0, 3/2, 1)	$\|1S, 3/2^+\rangle$	2765.9	2765.9(2.0)	2765	2772	2776	2745
(2, 0, 1/2, 1)	$\|2S, 1/2^+\rangle$	3171.2		3088	3164	3152	3164
(2, 0, 3/2, 1)	$\|2S, 3/2^+\rangle$	3180.5	3185.1(1.7) [18]	3123	3197	3190	3197
(3, 0, 1/2, 1)	$\|3S, 1/2^+\rangle$	3522.4		3489	3566		3561
(3, 0, 3/2, 1)	$\|3S, 3/2^+\rangle$	3523.6		3510	3571		3580
(1, 1, 1/2, 0)	$\|1P, 1/2^-\rangle$	3003.2	3000.41(0.22)	2966		2977	3041
(1, 1, 1/2, 1)	$\|1P, 1/2^-\rangle$	3010.7	3050.19(0.13)	3055		2990	3050
(1, 1, 3/2, 1)	$\|1P, 3/2^-\rangle$	3062.8	3065.54(0.26)	3029	3049	2986	3024
(1, 1, 3/2, 2)	$\|1P, 3/2^-\rangle$	3106.6	3090.10(0.5)	3054		2994	3033
(1, 1, 5/2, 2)	$\|1P, 5/2^-\rangle$	3145.3	3119.10(1.0)	3051	3055	3014	3010
(2, 1, 1/2, 0)	$\|2P, 1/2^-\rangle$	3414.3		3384			3427
(2, 1, 1/2, 1)	$\|2P, 1/2^-\rangle$	3421.3		3435			3436
(2, 1, 3/2, 1)	$\|2P, 3/2^-\rangle$	3436.8		3415	3408		3408
(2, 1, 3/2, 2)	$\|2P, 3/2^-\rangle$	3459.1		3433			3417
(2, 1, 5/2, 2)	$\|2P, 5/2^-\rangle$	3471.1		3427	3393		3393
(3, 1, 1/2, 0)	$\|3P, 1/2^-\rangle$	3731.3		3717			3813
(3, 1, 1/2, 1)	$\|3P, 1/2^-\rangle$	3737.2		3754			3823
(3, 1, 3/2, 1)	$\|3P, 3/2^-\rangle$	3745.7		3737	3732		3793
(3, 1, 3/2, 2)	$\|3P, 3/2^-\rangle$	3761.7		3752			3803
(3, 1, 5/2, 2)	$\|3P, 5/2^-\rangle$	3768.7		3744	3700		3777
(1, 2, 1/2, 1)	$\|1D, 1/2^+\rangle$	3289.7		3287			3354
(1, 2, 3/2, 1)	$\|1D, 3/2^+\rangle$	3323.5	3327.1(1.2) [18]	3282			3325
(1, 2, 3/2, 2)	$\|1D, 3/2^+\rangle$	3333.8	3327.1(1.2) [18]	3298			3335
(1, 2, 5/2, 3)	$\|1D, 5/2^+\rangle$	3364.1		3286	3360	3196	3299
(1, 2, 5/2, 2)	$\|1D, 5/2^+\rangle$	3396.5		3297			3308
(1, 2, 7/2, 3)	$\|1D, 7/2^+\rangle$	3422.9		3283	3314		3276

2.7 MeV higher than the model prediction for the $|1P, 3/2^-\rangle_{j=1}$ state; therefore, we simply give $J^P = \frac{3}{2}^-$ to the $\Omega_c(3065)^0$ state. Our theoretical predictions for $\Omega_c(3090)^0$ and $\Omega_c(3120)^0$ differ by 16 and 26 MeV, respectively, from their experimental masses. Accordingly, it is acceptable to assign them $J^P = \frac{3}{2}^-$ and $J^P = \frac{5}{2}^-$, respectively. The $|1P, 1/2^-\rangle_{j=1}$ state with $J^P = \frac{1}{2}^-$ is eventually identified as the $\Omega c(3050)^0$; however, its predicted mass is underestimated by 40 MeV. These five spin-parity assignments are also supported by Refs. [47,80]. Additionally, we predict the spin and parity of two newly discovered states $\Omega_c(3185)^0$ and $\Omega_c(3327)^0$. Our theoretical prediction for the $|2S, 3/2^+\rangle$ state is only 5 MeV less than the experimental mass of the $\Omega_c(3185)^0$ state, so we assign $J^P = \frac{3}{2}^+$ to the $\Omega_c(3185)^0$ state. Finally, since the experimentally measured mass of the $\Omega_c(3327)^0$ state only differs by a maximum of 6 MeV from our prediction for the $|1D, 3/2^+\rangle$ state, we assign $J^P = \frac{3}{2}^+$ to this state.

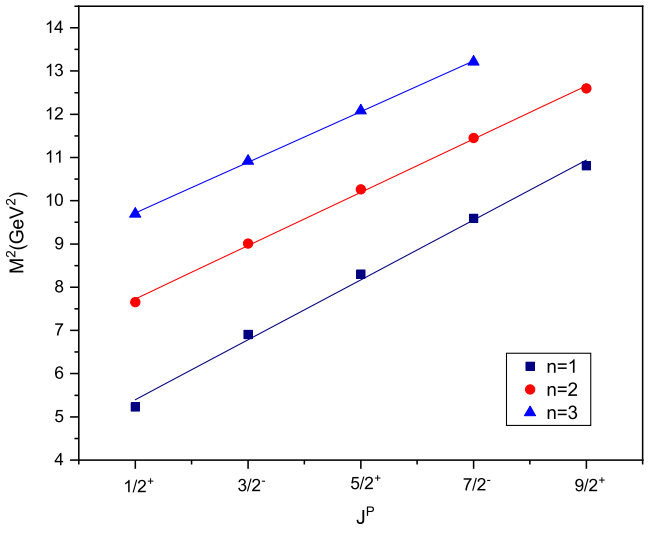

FIG. 2. Regge trajectory in the (J, M^2) plane for the Λ_c baryon for natural parity states.

Further, we compare our results with existing theoretical predictions made using the quark-diquark picture [23,26,44] and the three-body picture [20,25] of the baryon. Ebert *et al.* have studied the mass spectra of heavy baryons up to quite high excitations ($L = 5$, $n_r = 5$) using a QCD-motivated relativistic quark potential model with a quark-diquark picture of baryons [23]. We put their results in Tables III–VIII as a key reference for comparison with our results. For the Λ_c and Ξ_c baryons, our predictions are in

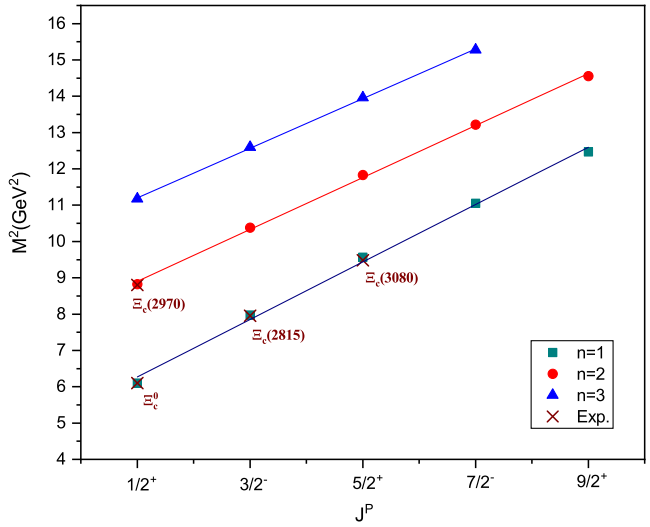

FIG. 3. Regge trajectory in the (J, M^2) plane for the Ξ_c baryon for natural parity states.

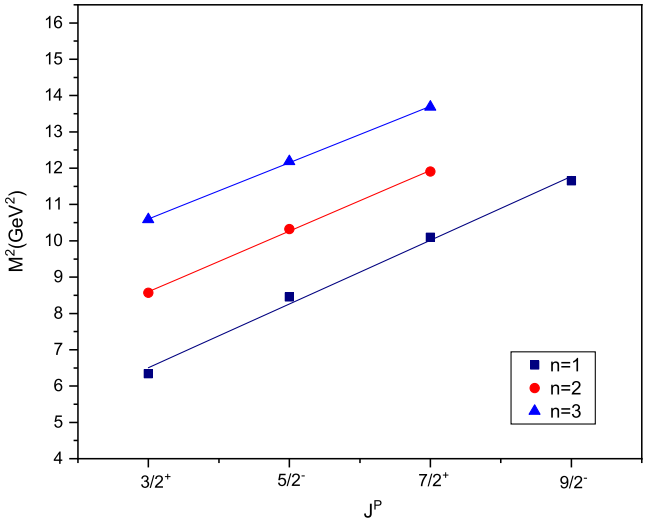

FIG. 5. Regge trajectory in the (J, M^2) plane for the Σ_c baryon for unnatural parity states.

excellent agreement with this reference. Up to the $3S$, $3P$, $3D$, $3F$, $2G$, and $1H$ states of the Λ_c baryon, our predictions differ by a maximum of 32.7 MeV only, and as we move to some more radially excited states, this difference slowly increases. For the Ξ_c baryon, our prediction for states up to $4S$, $4P$, $4D$, $3F$, $2G$, and $1H$ deviates from Ref. [23] at most by 61 MeV only. Our calculated masses for the Σ_c, Ξ_c', and Ω_c baryons are also consistent enough with Ref. [23] for states belonging to the S wave, P wave, and D wave. In Ref. [26], the nonrelativistic constituent quark model has been employed, and a quark-diquark picture has been considered to investigate the mass spectra of the Λ_c, Ξ_c, Σ_c, and Ξ_c' baryons. Our predictions and the results of this model are in accordance, although the difference rises for higher orbital and radial excited states. Chen *et al.* have investigated the mass spectra of the Λ_c and Ξ_c baryons in the quark-diquark framework [44] with the relativistic flux tube model. The spin-orbit interaction term in this work differs from our model since the Thomas-precession term is also included in our work, although its contribution is relatively small as it is inversely proportional to the square of the diquark's mass. The masses of the ground state and few excited states of singly charmed baryons were also studied in a three-body picture of the baryon with quark model in Ref. [20], and its findings are consistent with those of our model. We also compare our results for the Λ_c, Σ_c, and Ω_c baryons with Ref. [25] in which the hypercentral constituent quark model is employed with a three-body picture. This model's prediction for states belonging to a single orbital excitation

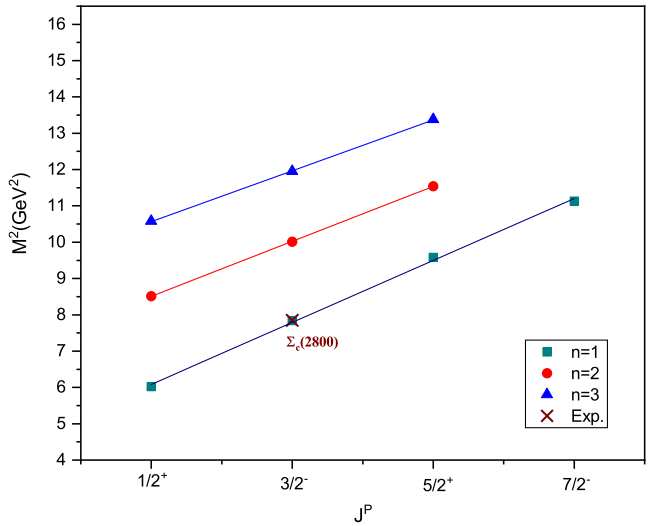

FIG. 4. Regge trajectory in the (J, M^2) plane for the Σ_c baryon for natural parity states.

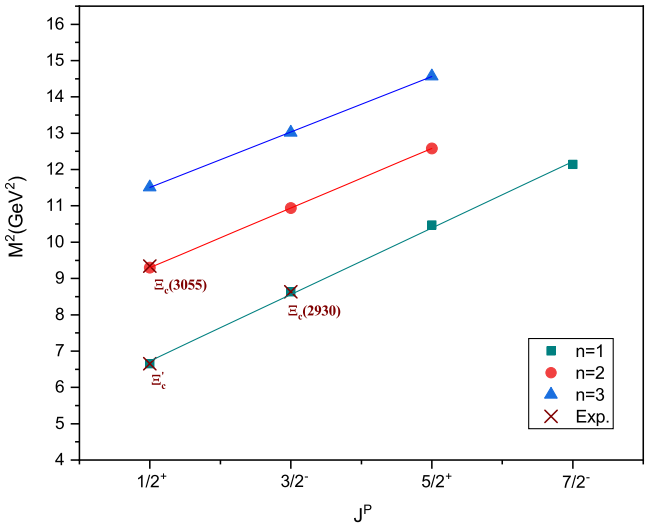

FIG. 6. Regge trajectory in the (J, M^2) plane for the Ξ_c' baryon for natural parity states.

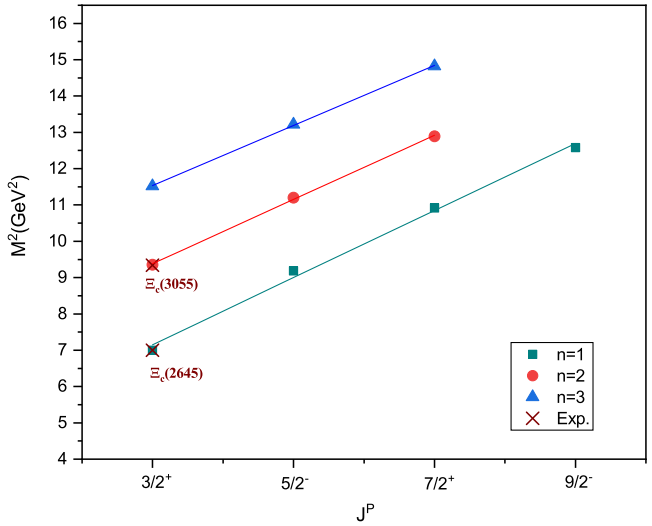

FIG. 7. Regge trajectory in the (J, M^2) plane for the Ξ_c' baryon for unnatural parity states.

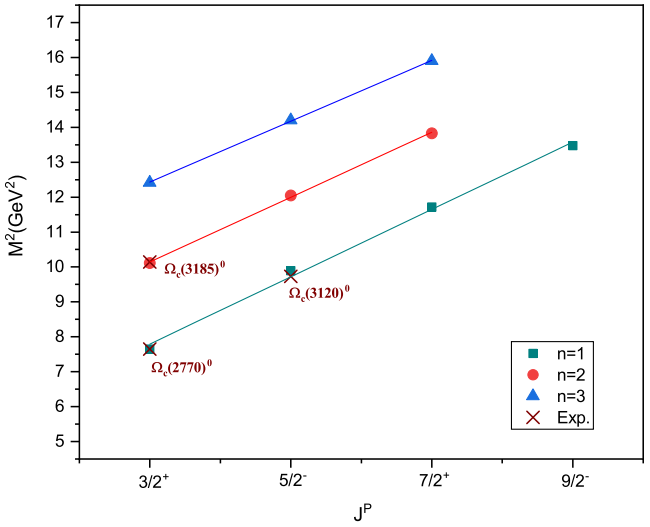

FIG. 9. Regge trajectory in the (J, M^2) plane for the Ω_c baryon for unnatural parity states.

is such that the state with a higher J lies below the state with a lower J, which is one of its limitations. However, no such inconsistency is seen in our model.

Since the masses of some the experimental candidates are quite close to more than one of our calculated masses, we have assigned more than one possible spin-parity quantum number to these experimental states. The most prominent way to eliminate some of these possibilities is to calculate the decay widths of these states. In Ref. [81], the authors linearly fitted the decay width (Γ) of the light mesons with the string length (rms) for maximal J states (where J = L + S1 + S2, and S1 and S2 are the spins of quark and antiquark, respectively) as

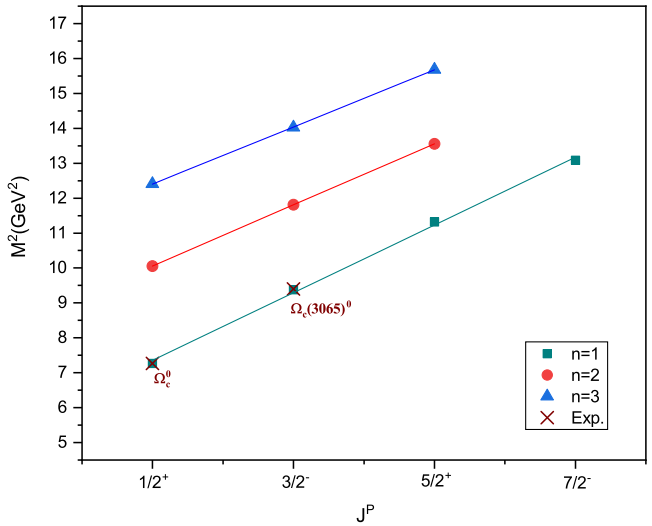

FIG. 8. Regge trajectory in the (J, M^2) plane for the Ω_c baryon for natural parity states.

$$\Gamma = \gamma(\mathrm{RMS} - r_0) \pm \Delta\Gamma, \tag{23}$$

where $\gamma = 0.05 \pm 0.01$ GeV^2 and $r_0 = 1.4 \pm 0.6$ GeV^{-1}. This linear relation is then extrapolated to glueballs. In our work, the total flux tube length is dependent on two quantum numbers, n and L [see Eq. (10)]. Now, to check whether such a linear relation between the decay width and the string length exists or not for singly charmed baryons, the experimental decay widths of at least three maximal J states are required. In the future, when sufficient experimental data on the decay width are available, the relation between the decay width and the string length can be studied to assign a spin-parity quantum number to singly charmed baryons.

IV. CONCLUSION

In this work, we used a mass formula derived from a relativistic flux tube model to investigate the mass spectra of singly charmed baryons in a heavy-quark–light-diquark framework. Because of the strong coupling between two light quarks, it is less probable that at the low-energy region, the baryon with an excited diquark could be detected, so we only considered states in which the diquark in the ground state excites orbitally or radially with respect to the charm quark, as these states are more likely to be detected first in the experiments. The spin-dependent interactions were included in the j-j coupling scheme. The experimentally well-known states of singly charmed baryons can be well reproduced, and their J^P values have also been confirmed by considering them as a system of a heavy quark and a light diquark connected by a mass-loaded flux tube. For low-lying orbital and radial excited states, our outcomes were consistent with many theoretical models, but for higher excited states, we observed a variety

of model-dependent differences. Our predicted mass spectra helped us assign the possible spin parity of experimentally detected states such as $\Sigma_c(2800)$, $\Xi_c(2923)$, $\Xi_c(2930)$, $\Xi_c(2970)$, $\Xi_c(3055)$, $\Xi_c(3080)$, and $\Xi_c(3123)$, as well as all five states of the Ω_c baryon, including $\Omega_c(3000)$, $\Omega_c(3050)$, $\Omega_c(3065)$, $\Omega_c(3090)$, and $\Omega_c(3119)$. We also predicted many unobserved states of singly charmed baryons which have good potential to be detected first in the experiment. These predictions can be used as reference data for upcoming experimental searches like CMS, LHCb, Belle II, BESIII [82], and PANDA [83] for heavy hadron physics.

Despite the fact that we employed a quark-diquark picture, the possibility of a three-body picture of a singly charmed baryon may not be removed. The three-body relativistic flux tube model has also been obtained in Ref. [70] from the Wilson area law in QCD, but for a three-body system it is very difficult to obtain the Regge relation between the mass and angular momentum. Therefore, utilizing the three-body relativistic flux tube model to describe the mass spectra of singly charmed baryons remains an open problem. Additionally, due to this, we were unable to find a connection between the two-body and three-body flux tube model, and it is still not clear how the quark-diquark relativistic flux tube develops from the three-body relativistic flux tubes.

After the successful determination of the mass spectra of singly charmed baryons, we will extend this model to study singly bottom, doubly and triply charmed, and bottom baryons.

ACKNOWLEDGMENTS

P. J. acknowledges the financial assistance from the Council of Scientific & Industrial Research under the JRF-FELLOWSHIP scheme with File No. 09/1007 (13321)/2022-EMR-I.

APPENDIX

Here, we go into detail on how to obtain mass-splitting operators that are involved in spin-dependent interactions for singly charmed baryons with a vector diquark only. The following outlines only three orbitally excited states for demonstration purposes.

(1) The S wave: For this state, $L = 0$. In spin-dependent interactions, only spin-spin contact hyperfine interactions survive. The expectation value of $\mathbf{S_d}.\mathbf{S_c}$, in both the L-S and j-j coupling is the same.

(2) The P wave: We have three angular momentum vectors $\mathbf{S_d}$, $\mathbf{S_c}$, and $\mathbf{L}$. In the L-S coupling scheme, $\mathbf{S_d}$ and $\mathbf{S_c}$ first couple to give $\mathbf{S}$. The simultaneous eigenstate of $\mathbf{S}$ and its third component S_3 can be constructed from uncoupled states $|S_d, S_{d_3}\rangle$ and $|S_c, S_{c_3}\rangle$ as [84]

$$|S_d S_c; S\ S_3\rangle = \sum_{S_{d_3} S_{c_3}} C^{S_d S_c S}_{S_{d_3} S_{c_3} S_3} |S_d S_{d_3}\rangle |S_c S_{c_3}\rangle. \tag{A1}$$

Then, $\mathbf{S}$ combines with $\mathbf{L}$ to generate total angular momentum $\mathbf{J}$. The simultaneous eigenstate of $\mathbf{J}$, J_3, and $\mathbf{S}$ can be formed by $|S_d S_c; S\ S_3\rangle$ and the uncoupled state $|L\ L_3\rangle$ as

$$\begin{aligned} |(S_d S_c) SL; J\ J_3\rangle &= \sum_{S_3 L_3} C^{SLJ}_{S_3 L_3 J_3} |S_d S_c; S\ S_3\rangle |L\ L_3\rangle \\ &= \sum_{S_{d_3} S_{c_3} L_3 S_3} C^{S_d S_c S}_{S_{d_3} S_{c_3} S_3} C^{SLJ}_{S_3 L_3 J_3} |S_d S_{d_3}\rangle |S_c S_{c_3}\rangle |L\ L_3\rangle, \end{aligned} \tag{A2}$$

where $C^{S_d S_c S}_{S_{d_3} S_{c_3} S_3}$ and $C^{SLJ}_{S_3 L_3 J_3}$ are Clebsch-Gordan coefficients. S_{d_3}, S_{c_3}, L_3, and J_3 denote the third component of the respective angular momentum. For simplicity, we abbreviate the basis $|(S_d S_c) SL; J\, J_3\rangle$ as $|^{2S+1}L_J; J_3\rangle$, and the product states $|S_d S_{d_3}\rangle |S_c S_{c_3}\rangle |L\, L_3\rangle$ as $|S_{d_3}, S_{c_3}, L_3\rangle$ for fixed values of S_d, , S_c and L. Then, the L-S coupling basis states can be constructed as a linear combination of the $|S_{d_3}, S_{c_3}, L_3\rangle$ states using

$$|^{2S+1}L_J; J_3\rangle = \sum_{S_{d_3} S_{c_3} L_3 S_3} C^{S_d S_c S}_{S_{d_3} S_{c_3} S_3} C^{SLJ}_{S_3 L_3 J_3} |S_{d_3}, S_{c_3}, L_3\rangle. \tag{A3}$$

Finally, utilizing the above relation, the L-S bases are constructed for the P waves which are listed below [85]:

$$|^2P_{1/2}; 1/2\rangle = -\frac{\sqrt{2}}{3}\left|0, -\frac{1}{2}, 1\right\rangle + \frac{\sqrt{2}}{3}\left|1, -\frac{1}{2}, 0\right\rangle + \frac{2}{3}\left|-1, \frac{1}{2}, 1\right\rangle - \frac{1}{3}\left|0, \frac{1}{2}, 0\right\rangle, \tag{A4}$$

$$|^4P_{1/2};1/2\rangle = \frac{1}{3}\left|0,-\frac{1}{2},1\right\rangle - \frac{1}{3}\left|1,-\frac{1}{2},0\right\rangle + \frac{1}{3\sqrt{2}}\left|-1,\frac{1}{2},1\right\rangle - \frac{\sqrt{2}}{3}\left|0,\frac{1}{2},0\right\rangle + \frac{1}{\sqrt{2}}\left|1,\frac{1}{2},-1\right\rangle, \tag{A5}$$

$$|^2P_{3/2};3/2\rangle = \sqrt{\frac{2}{3}}\left|1,-\frac{1}{2},1\right\rangle - \frac{1}{\sqrt{3}}\left|0,\frac{1}{2},1\right\rangle, \tag{A6}$$

$$|^4P_{3/2};3/2\rangle = -\sqrt{\frac{2}{15}}\left|1,-\frac{1}{2},1\right\rangle - \frac{2}{\sqrt{15}}\left|0,\frac{1}{2},1\right\rangle + \sqrt{\frac{3}{5}}\left|1,\frac{1}{2},0\right\rangle, \quad \text{and} \tag{A7}$$

$$|^4P_{5/2};5/2\rangle = \left|1,\frac{1}{2},1\right\rangle. \tag{A8}$$

Now we define the operators involved in spin-dependent interactions. The operator $\mathbf{L}.\mathbf{S_i}$ in terms of a raising and lowering operator is given by

$$\mathbf{L}.\mathbf{S_i} = \frac{1}{2}[L_+S_{i-} + L_-S_{i+}] + L_3S_{i3}, \tag{A9}$$

where i = l or h. The operator engaged in the tensor interaction term can be simplified to [47]

$$\hat{B} = \frac{-3}{(2L-1)(2L+3)}\left[(\mathbf{L}.\mathbf{S_d})(\mathbf{L}.\mathbf{S_c}) + (\mathbf{L}.\mathbf{S_c})(\mathbf{L}.\mathbf{S_d}) - \frac{2}{3}L(L+1)(\mathbf{S_d}.\mathbf{S_c})\right]. \tag{A10}$$

Squaring the identity $\mathbf{S} = \mathbf{S_d} + \mathbf{S_c}$ allows one to calculate the expectation value of the operator $\mathbf{S_d}.\mathbf{S_c}$ as

$$\langle \mathbf{S_d}.\mathbf{S_c}\rangle = \frac{1}{2}[S(S+1) - S_d(S_d+1) - S_c(S_c+1)]. \tag{A11}$$

With these operators in hand, we determine their expectation values in the L-S basis $[^2P_J, ^4P_J]$ for different possible values of J as listed below: For J = 1/2,

$$\langle \mathbf{L}.\mathbf{S_d}\rangle = \begin{bmatrix} -\frac{4}{3} & -\frac{\sqrt{2}}{3} \\ -\frac{\sqrt{2}}{3} & -\frac{5}{3} \end{bmatrix}, \quad \langle \mathbf{L}.\mathbf{S_c}\rangle = \begin{bmatrix} \frac{1}{3} & \frac{\sqrt{2}}{3} \\ \frac{\sqrt{2}}{3} & -\frac{5}{6} \end{bmatrix}, \quad \langle \hat{B}\rangle = \begin{bmatrix} 0 & \frac{1}{\sqrt{2}} \\ \frac{1}{\sqrt{2}} & -1 \end{bmatrix}, \quad \langle \mathbf{S_d}.\mathbf{S_c}\rangle = \begin{bmatrix} -1 & 0 \\ 0 & \frac{1}{2} \end{bmatrix}. \tag{A12}$$

For J = 3/2,

$$\langle \mathbf{L}.\mathbf{S_d}\rangle = \begin{bmatrix} \frac{2}{3} & -\frac{\sqrt{5}}{3} \\ -\frac{\sqrt{5}}{3} & -\frac{2}{3} \end{bmatrix}, \quad \langle \mathbf{L}.\mathbf{S_c}\rangle = \begin{bmatrix} -\frac{1}{6} & \frac{\sqrt{5}}{3} \\ \frac{\sqrt{5}}{3} & -\frac{1}{3} \end{bmatrix}, \quad \langle \hat{B}\rangle = \begin{bmatrix} 0 & -\frac{1}{2\sqrt{5}} \\ -\frac{1}{2\sqrt{5}} & \frac{4}{5} \end{bmatrix}, \quad \langle \mathbf{S_d}.\mathbf{S_c}\rangle = \begin{bmatrix} -1 & 0 \\ 0 & \frac{1}{2} \end{bmatrix}. \tag{A13}$$

For J = 5/2,

$$\langle \mathbf{L}.\mathbf{S_d}\rangle = 1, \quad \langle \mathbf{L}.\mathbf{S_c}\rangle = \frac{1}{2}, \quad \langle \hat{B}\rangle = -\frac{1}{5}, \quad \langle \mathbf{S_d}.\mathbf{S_c}\rangle = \frac{1}{2}. \tag{A14}$$

As $m_c \gg m_d$, the term proportional to $L.S_d$ dominates over other terms involved in spin-dependent interactions. The $L.S_d$ matrix is diagonal in the $|J,j\rangle$ basis in the j-j coupling. Therefore, it is reasonable to employ the $|J,j\rangle$ basis where the dominant interaction is diagonal and the other interactions are treated perturbatively. For each eigenvalue λ of $L.S_d$ with specific J, we find the corresponding eigenvector, which forms the $|J,j\rangle$ basis as listed below:

$$\lambda = -2\text{:} \ \left|\mathrm{J} = \frac{1}{2}, \mathrm{j} = 0\right\rangle = \frac{1}{\sqrt{3}}|^2P_{1/2}\rangle + \sqrt{\frac{2}{3}}|^4P_{1/2}\rangle, \tag{A15}$$

$$\lambda=-1\colon\ \left|\mathrm{J}=\frac{1}{2},\mathrm{j}=1\right\rangle=-\sqrt{\frac{2}{3}}|^2P_{1/2}\rangle+\frac{1}{\sqrt{3}}|^4P_{1/2}\rangle, \tag{A16}$$

$$\lambda=-1\colon\ \left|\mathrm{J}=\frac{3}{2},\mathrm{j}=1\right\rangle=\frac{1}{\sqrt{6}}|^2P_{3/2}\rangle+\sqrt{\frac{5}{6}}|^4P_{3/2}\rangle, \tag{A17}$$

$$\lambda=1\colon\ \left|\mathrm{J}=\frac{3}{2},\mathrm{j}=2\right\rangle=-\sqrt{\frac{5}{6}}|^2P_{3/2}\rangle+\frac{1}{\sqrt{6}}|^4P_{3/2}\rangle, \tag{A18}$$

$$\left|\mathrm{J}=\frac{5}{2},\mathrm{j}=2\right\rangle=|^4P_{5/2}\rangle. \tag{A19}$$

This gives the baryonic states in the heavy-quark limit. Now, we determine the expectation value for each mass-splitting operator in the $|J,j\rangle$ basis and list the results in Table II.

(3) The D wave: For the D wave, the same process as for the P wave is used to produce the mass-splitting operators. We first use Eq. (A3) to construct the L-S basis and the outcomes are

$$\begin{aligned}|^4D_{1/2};1/2\rangle=&-\sqrt{\frac{2}{5}}\left|-1,-\frac{1}{2},2\right\rangle+\frac{1}{\sqrt{5}}\left|0,-\frac{1}{2},1\right\rangle-\frac{1}{\sqrt{15}}\left|1,-\frac{1}{2},0\right\rangle+\frac{1}{\sqrt{10}}\left|-1,\frac{1}{2},1\right\rangle\\&-\sqrt{\frac{2}{15}}\left|0,\frac{1}{2},0\right\rangle+\frac{1}{\sqrt{10}}\left|1,\frac{1}{2},-1\right\rangle,\end{aligned} \tag{A20}$$

$$|^2D_{3/2};3/2\rangle=-\frac{2}{\sqrt{15}}\left|0,-\frac{1}{2},2\right\rangle+\sqrt{\frac{2}{15}}\left|1,-\frac{1}{2},1\right\rangle+2\sqrt{\frac{2}{15}}\left|-1,\frac{1}{2},2\right\rangle-\frac{1}{\sqrt{15}}\left|0,\frac{1}{2},1\right\rangle, \tag{A21}$$

$$|^4D_{3/2};3/2\rangle=\frac{2}{\sqrt{15}}\left|0,-\frac{1}{2},2\right\rangle-\sqrt{\frac{2}{15}}\left|1,-\frac{1}{2},1\right\rangle+\sqrt{\frac{2}{15}}\left|-1,\frac{1}{2},2\right\rangle-\frac{2}{\sqrt{15}}\left|0,\frac{1}{2},1\right\rangle+\frac{1}{\sqrt{5}}\left|1,\frac{1}{2},0\right\rangle, \tag{A22}$$

$$|^2D_{5/2};5/2\rangle=\sqrt{\frac{2}{3}}\left|1,-\frac{1}{2},2\right\rangle-\frac{1}{\sqrt{3}}\left|0,\frac{1}{2},2\right\rangle, \tag{A23}$$

$$|^4D_{5/2};5/2\rangle=-\frac{2}{\sqrt{21}}\left|1,-\frac{1}{2},2\right\rangle-2\sqrt{\frac{2}{21}}\left|0,\frac{1}{2},2\right\rangle+\sqrt{\frac{3}{7}}\left|1,\frac{1}{2},1\right\rangle,\quad\text{and} \tag{A24}$$

$$|^4D_{7/2};7/2\rangle=\left|1,\frac{1}{2},2\right\rangle. \tag{A25}$$

Second, the expectation of the mass-splitting operators for specific J in the L-S basis $[^2D_J,{}^4D_J,]$ is computed and listed below.

For $\mathrm{J}=1/2$,

$$\langle\mathbf{L}.\mathbf{S_d}\rangle=-3,\qquad\langle\mathbf{L}.\mathbf{S_c}\rangle=-\frac{3}{2},\qquad\langle\hat{B}\rangle=-1,\qquad\langle\mathbf{S_d}.\mathbf{S_c}\rangle=\frac{1}{2}. \tag{A26}$$

For $\mathrm{J}=3/2$,

$$\langle\mathbf{L}.\mathbf{S_d}\rangle=\begin{bmatrix}-2&-1\\-1&-2\end{bmatrix},\qquad\langle\mathbf{L}.\mathbf{S_c}\rangle=\begin{bmatrix}\frac{1}{2}&1\\1&-1\end{bmatrix},\qquad\langle\hat{B}\rangle=\begin{bmatrix}0&\frac{1}{2}\\\frac{1}{2}&0\end{bmatrix},\qquad\langle\mathbf{S_d}.\mathbf{S_c}\rangle=\begin{bmatrix}-1&0\\0&\frac{1}{2}\end{bmatrix}. \tag{A27}$$

For $J = 5/2$,

$$\langle \mathbf{L}.\mathbf{S_d} \rangle = \begin{bmatrix} \frac{4}{3} & -\frac{\sqrt{14}}{3} \\ -\frac{\sqrt{14}}{3} & -\frac{1}{3} \end{bmatrix}, \qquad \langle \mathbf{L}.\mathbf{S_c} \rangle = \begin{bmatrix} -\frac{1}{3} & \frac{\sqrt{14}}{3} \\ \frac{\sqrt{14}}{3} & -\frac{1}{6} \end{bmatrix}, \qquad \langle \hat{B} \rangle = \begin{bmatrix} 0 & -\frac{1}{\sqrt{14}} \\ -\frac{1}{\sqrt{14}} & \frac{5}{7} \end{bmatrix}, \qquad \langle \mathbf{S_d}.\mathbf{S_c} \rangle = \begin{bmatrix} -1 & 0 \\ 0 & \frac{1}{2} \end{bmatrix}. \tag{A28}$$

For $J = 7/2$,

$$\langle \mathbf{L}.\mathbf{S_d} \rangle = 2, \qquad \langle \mathbf{L}.\mathbf{S_c} \rangle = 1, \qquad \langle \hat{B} \rangle = -\frac{2}{7}, \qquad \langle \mathbf{S_d}.\mathbf{S_c} \rangle = \frac{1}{2}. \tag{A29}$$

In the third step, the eigenvalue λ and the eigenvector of $\langle \mathbf{L}.\mathbf{S_d} \rangle$ are determined, and the $|J, j\rangle$ basis is constructed as a linear combination of the L-S basis with coefficients depending on the eigenvector of $\langle \mathbf{L}.\mathbf{S_d} \rangle$,

$$\left| \mathrm{J} = \frac{1}{2}, \mathrm{j} = 1 \right\rangle = |^4D_{1/2}\rangle, \tag{A30}$$

$$\lambda = -3: \left| \mathrm{J} = \frac{3}{2}, \mathrm{j} = 1 \right\rangle = \frac{1}{\sqrt{2}} |^2D_{3/2}\rangle + \frac{1}{\sqrt{2}} |^4D_{3/2}\rangle, \tag{A31}$$

$$\lambda = -1: \left| \mathrm{J} = \frac{3}{2}, \mathrm{j} = 2 \right\rangle = -\frac{1}{\sqrt{2}} |^2D_{3/2}\rangle + \frac{1}{\sqrt{2}} |^4D_{3/2}\rangle, \tag{A32}$$

$$\lambda = 2: \left| \mathrm{J} = \frac{5}{2}, \mathrm{j} = 2 \right\rangle = -\frac{\sqrt{7}}{3} |^2D_{5/2}\rangle + \frac{\sqrt{2}}{3} |^4D_{5/2}\rangle, \tag{A33}$$

$$\lambda = -1: \left| \mathrm{J} = \frac{5}{2}, \mathrm{j} = 3 \right\rangle = \frac{\sqrt{2}}{3} |^2D_{5/2}\rangle + \frac{\sqrt{7}}{3} |^4D_{5/2}\rangle, \tag{A34}$$

$$\left| \mathrm{J} = \frac{7}{2}, \mathrm{j} = 3 \right\rangle = |^4D_{7/2}\rangle. \tag{A35}$$

Finally, we find the expectation value of the mass-splitting operators in the $|J, j\rangle$ basis and collect our results in Table II.

[1] R. L. Workman *et al.* (Particle Data Group), Prog. Theor. Exp. Phys. **2022**, 083C01 (2022).
[2] M. Artuso *et al.* (CLEO Collaboration), Phys. Rev. Lett. **86**, 4479 (2001).
[3] K. Abe *et al.* (Belle Collaboration), Phys. Rev. Lett. **98**, 262001 (2007).
[4] K. Tanida and for the Belle Collaboration, Hadron Spectroscopy and Structure (2020), p. 183.
[5] B. Aubert *et al.* (*BABAR* Collaboration), Phys. Rev. D **77**, 012002 (2008).
[6] Y. Kato *et al.* (Belle Collaboration), Phys. Rev. D **89**, 052003 (2014).
[7] R. Chistov *et al.* (Belle Collaboration), Phys. Rev. Lett. **97**, 162001 (2006).
[8] R. Aaij *et al.* (LHCb Collaboration), Phys. Rev. Lett. **124**, 222001 (2020).
[9] Y. B. Li *et al.* (Belle Collaboration), Eur. Phys. J. C **78**, 928 (2018).
[10] Y. B. Li *et al.* (Belle Collaboration), Eur. Phys. J. C **78**, 252 (2018).
[11] B. Aubert *et al.* (*BABAR* Collaboration), Phys. Rev. D **77**, 031101 (2008).
[12] J. Yelton *et al.* (Belle Collaboration), Phys. Rev. D **94**, 052011 (2016).

[13] T. J. Moon *et al.* (Belle Collaboration), Phys. Rev. D **103**, L111101 (2021).
[14] R. Mizuk *et al.* (Belle Collaboration), Phys. Rev. Lett. **94**, 122002 (2005).
[15] B. Aubert *et al.* (*BABAR* Collaboration), Phys. Rev. D **78**, 112003 (2008).
[16] R. Aaij *et al.* (LHCb Collaboration), Phys. Rev. Lett. **118**, 182001 (2017).
[17] J. Yelton *et al.* (Belle Collaboration), Phys. Rev. D **97**, 051102 (2018).
[18] LHCb Collaboration, arXiv:2302.04733v1.
[19] H. Garcilazo, J. Vijande, and A. Valcarce, J. Phys. G **34**, 961 (2007).
[20] W. Roberts and M. Pervin, Int. J. Mod. Phys. A **23**, 19 (2008).
[21] A. Valcarce, H. Garcilazo, and J. Vijande, Eur. Phys. J. A **37**, 217 (2008).
[22] D. Ebert, R. N. Faustov, and V. O. Galkin, Phys. Lett. B **659**, 612 (2008).
[23] D. Ebert, R. N. Faustov, and V. O. Galkin, Phys. Rev. D **84**, 014025 (2011).
[24] T. Yoshida, E. Hiyama, A. Hosaka, M. Oka, and K. Sadato, Phys. Rev. D **92**, 114029 (2015).
[25] Z. Shah, K. Thakkar, A. K. Rai, and P. C. Vinodkumar, Eur. Phys. J. A **52**, 313 (2016).
[26] B. Chen, K. W. Wei, X. Liu, and T. Matsuki, Eur. Phys. J. C **77**, 154 (2017).
[27] K. L. Wang, Q. F. Lü, and X. H. Zhong, Phys. Rev. D **100**, 114035 (2019).
[28] S. Q. Luo and X. Liu, arXiv:2306.04588v1.
[29] H. Y. Cheng and C. K. Chua, Phys. Rev. D **75**, 014006 (2007).
[30] H. Y. Cheng and C. K. Chua, Phys. Rev. D **92**, 074014 (2015).
[31] Y. Kawakami and M. Harada, Phys. Rev. D **99**, 094016 (2019).
[32] P. Perez-Rubio, S. Collins, and G. S. Bali, Phys. Rev. D **92**, 034504 (2015).
[33] H. X. Chen, Q. Mao, W. Chen, A. Hosaka, X. Liu, and S. L. Zhu, Phys. Rev. D **95**, 094008 (2017).
[34] J. R. Zhang and M. Q. Huang, Phys. Rev. D **77**, 094002 (2008).
[35] J. R. Zhang and M. Q. Huang, Phys. Rev. D **78**, 094015 (2008).
[36] Z. G. Wang, Eur. Phys. J. C **68**, 479 (2010).
[37] Z. G. Wang, Eur. Phys. J. A **47**, 81 (2011).
[38] H. X. Chen, Q. Mao, A. Hosaka, X. Liu, and S. L. Zhu, Phys. Rev. D **94**, 114016 (2016).
[39] Q. Mao, H. X. Chen, A. Hosaka, X. Liu, and S. L. Zhu, Phys. Rev. D **96**, 074021 (2017).
[40] Z. G. Wang, Nucl. Phys. **B926**, 467 (2018).
[41] Z. G. Wang, Chin. Phys. C **45**, 013109 (2021).
[42] J. Oudichhya, K. Gandhi, and A. K. Rai, Phys. Rev. D **103**, 114030 (2021).
[43] D.-X. Wang, B. Chen, and A. Zhang, Chin. Phys. C **35**, 525 (2011).
[44] B. Chen, K. W. Wei, and A. Zhang, Eur. Phys. J. A **51**, 82 (2015).
[45] D. Jia, W. N. Liu, and A. Hosaka, Phys. Rev. D **101**, 034016 (2020).
[46] E. Jenkins, Phys. Rev. D **54**, 4515 (1996).
[47] M. Karliner and J. L. Rosner, Phys. Rev. D **95**, 114012 (2017).
[48] N. Isgur and J. Paton, Phys. Rev. D **31**, 2910 (1985).
[49] D. LaCourse and M. G. Olsson, Phys. Rev. D **39**, 2751 (1989).
[50] C. Olson, M. G. Olsson, and K. Williams, Phys. Rev. D **45**, 4307 (1992).
[51] M. G. Olsson and K. Williams, Phys. Rev. D **48**, 417 (1993).
[52] C. Olson, M. G. Olsson, and D. LaCourse, Phys. Rev. D **49**, 4675 (1994).
[53] M. G. Olsson, Nuovo Cimento A **107**, 2541 (1994).
[54] M. G. Olsson and S. Vesseli, Phys. Rev. D **51**, 3578 (1995).
[55] M. G. Olsson, S. Vesseli, and K. Wikkiams, Phys. Rev. D **53**, 4006 (1996).
[56] T. J. Allen, M. G. Olsson, and S. Vesseli, Phys. Rev. D **60**, 074026 (1999).
[57] Y. Nambu, Phys. Rev. D **10**, 4262 (1974).
[58] F. Buissereti, Phys. Rev. C **76**, 025206 (2007).
[59] B. Chen, D.-X. Wang, and A. Zhang, Phys. Rev. D **80**, 071502 (2009).
[60] H.-Y. Shan and A.-L. Zhang, Chin. Phys. C **34**, 16 (2010).
[61] T. J. Burns, F. Piccinini, A. D. Polosa, and C. Sabelli, Phys. Rev. D **82**, 074003 (2010).
[62] D. Jia and W.-C. Dong, Eur. Phys. J. Plus **134**, 123 (2019).
[63] B. Chen, A. Zhang, and J. He, Phys. Rev. D **101**, 014020 (2020).
[64] B. Chen, D.-X. Wang, and A. Zhang, Chin. Phys. C **33**, 1327 (2009).
[65] Y.-X. Song, D. Jia, W.-X. Zhang, and A. Hosaka, Eur. Phys. J. C **83**, 1 (2023).
[66] M. Iwasaki, S.-I. Nawa, T. Sanada, and F. Takagi, Phys. Rev. D **68**, 074007 (2003).
[67] M. Iwasaki and F. Takagi, Phys. Rev. D **77**, 054020 (2008).
[68] F. Buisseret, V. Mathieu, and C. Semay, Phys. Rev. D **80**, 074021 (2009).
[69] H. Nandan and A. Ranjan, Int. J. Mod. Phys. A **31**, 1650007 (2016).
[70] N. Brambilla, G. M. Prosperi, and A. Vairo, Phys. Lett. B **362**, 113 (1995).
[71] N. Isgur and M. B. Wise, Phys. Rev. Lett. **66**, 1130 (1991).
[72] G. Hooft, arXiv:hep-th/0408148v1.
[73] C. Semay, F. Buisseret, and F. Stancu, Phys. Rev. D **78**, 076003 (2008).
[74] I. M. Narodetskii, M. A. Trusov, and A. I. Veselov, Phys. At. Nucl. **72**, 536 (2009).
[75] B. Chen, S. Q. Luo, K. W. Wei, and X. Liu, Phys. Rev. D **105**, 074014 (2022).
[76] A. Selem and F. Wilczek, in *Proceedings of the New Trends in HERA Physics* (2005), p. 337, 10.1142/6116.
[77] A. K. Rai, B. Patel, and P. C. Vinodkumar, Phys. Rev. C **78**, 055202 (2008).
[78] K. Chen, Y. Dong, X. Liu, Q.-F. Lü, and T. Matsuki, Eur. Phys. J. C **78**, 20 (2018).
[79] G.-L. Yu *et al.*, Nucl. Phys. **B990**, 116183 (2023).

[80] D. Jia, J.-H. Pan, and C.-Q. Pang, Eur. Phys. J. C **81**, 434 (2021).
[81] E. Abreu and P. Bicudo, J. Phys. G **34**, 195207 (2007).
[82] H. B. Li *et al.* (BESIII Collaboration), arXiv:2204.08943v1.
[83] G. Barucca *et al.* (PANDA Collaboration), Eur. Phys. J. A **57**, 184 (2021).
[84] D. M. Brink and G. R. Satchler, *Angular Momentum* (Clarendon Press, Oxford, 1968), p. 40.
[85] M. Karliner and J. L. Rosner, Phys. Rev. D **92**, 074026 (2015).